VVA-based combustion control strategies for efficiency improvement and emissions control in a heavy-duty diesel engine

Wei Guan[1], Vinícius B. Pedrozo[1], Hua Zhao[1],

[1]Brunel University London, UK;

Zhibo Ban[2], Tiejian Lin[2]

[2]Guangxi Yuchai Machinery Company, China

Abstract

High nitrogen oxide (NOx) levels of the conventional diesel engine combustion often requires the introduction of exhaust gas recirculation (EGR) at high engine loads. This can adversely affect the smoke emissions and fuel conversion efficiency associated with a reduction of the in-cylinder air-fuel ratio (lambda). In addition, low exhaust gas temperatures (EGT) at low engine loads reduce the effectiveness of aftertreatment systems (ATS) necessary to meet stringent emissions regulations. These are some of the main issues encountered by current heady-duty (HD) diesel engines. In this work, variable valve actuation (VVA)-based advanced combustion control strategies have been researched as means of improving upon the engine exhaust temperature, emissions, and efficiency. Experimental analysis was carried out on a single-cylinder HD diesel engine equipped with a high pressure common rail fuel injection system, a high-pressure loop cooled EGR, and a VVA system. The VVA system enables a late intake valve closing (LIVC) and a second intake valve opening (2IVO) during the exhaust stroke.

The results showed that Miller cycle was an effective technology for exhaust temperature management of low engine load operations, increasing the EGT by 40°C and 75°C when running engine at 2.2 and 6 bar net indicated mean effective pressure (IMEP), respectively. However, Miller cycle adversely effected carbon monoxide (CO) and unburned hydrocarbon (HC) emissions at a light load of 2.2 bar IMEP. This could be overcome when combing Miller cycle with a 2IVO strategy due to the formation of a relatively hotter in-cylinder charge induced by the presence of internal EGR (iEGR). This strategy also led to a significant reduction in soot emissions by 82% when compared to the baseline engine operation. Alternatively, the use of external EGR and post injection on a Miller cycle operation decreased NOx emissions by 67% at a part load of 6 bar IMEP. This contributed to a reduction of 2.2% in the total fluid consumption, which takes into account the urea consumption in ATS. At a high engine load of 17 bar IMEP, a highly boosted Miller cycle strategy with EGR increased the fuel conversion efficiency by 1.5% while reducing the total fluid consumption by 5.4%. The overall results demonstrated that advanced VVA-based combustion control strategies can control the EGT and engine-out emissions at low engine loads as well as improve upon the fuel conversion efficiency and total fluid consumption at high engine loads, potentially reducing the engine operational costs.

Keywords

Heavy-duty diesel engine, VVA, Miller cycle, EGR, post injection, total fluid consumption, exhaust gas temperature

1. Introduction

Over the last two decades, the research and development of heavy-duty diesel engines have been focused on the reduction of the NOx and particulate matter (PM) emissions. Their formation is due to the fact that conventional diesel engine combustion is characterised by a wide range of local in-cylinder gas temperatures and equivalence ratios as a result of the non-premixed diffusion-controlled combustion [1]. More recently, the demand for the reduction of fuel consumption and carbon dioxide (CO_2) coupled with the customer's requirements to reduce the vehicle operational cost also impose stringent requirements on the development of HD diesel engines [2,3]. To address these issues, in-cylinder combustion control technologies combined with emission control ATS is required [4,5].

Low temperature combustion (LTC) modes, such as Homogeneous Charge Compression Ignition (HCCI), Premixed Charge Compression Ignition (PCCI), and Partially Premixed Charge Compression Ignition (PPCI), have shown their potential to achieve simultaneous low NOx and soot emissions. However, these combustion modes suffer from high unburned HC and CO emissions, lack of combustion phasing control and limited load range [6–8]. Moreover, these LTC strategies result in significantly lower exhaust gas temperature, which creates great challenges for the effective operation of the ATS including selective catalytic reduction (SCR), diesel particulate filter (DPF), and diesel oxidation catalyst (DOC) at the low engine loads and cold-start [9]. These ATS are strongly dependent on the exhaust gas temperature (EGT) and a minimum EGT of approximately 200°C is required for catalyst light-off and to initiate the emissions control [10]. When the EGT is above 300°C, the unburned HC and CO emissions can be effectively removed from the exhaust gases in the DOC [11]. Additionally, the active regeneration of the DPF can be realised when the inlet gas temperature reaches 500°C [12]. Advanced combustion technologies such as multiple fuel injection strategy, higher fuel injection pressure, and higher boost pressure have been employed to improve upon fuel conversion efficiency, however, these technologies are typically accompanied with a lower EGT [13].

Alternatively, the application of VVA-based technology such as Miller cycle and iEGR to diesel engines has been shown as an effective technology for exhaust emissions and EGT control. This is due to the fact that Miller cycle achieved via early or late intake valve closing (IVC) timings reduces the peak in-cylinder combustion temperature and air-fuel ratio. The iEGR realised via a 2IVO during exhaust stroke and/or exhaust valve re-opening (2EVO) during intake stroke allows for the control of the in-cylinder hot residual gas fraction [14,15].

Gonca et al. [16] evaluated the effect of Miller cycle operation on engine performance and exhaust emissions by means of experimental and simulation analysis. The lower effective compression ratio (ECR) led to a reduction of 30% in NOx emissions at the expense of lower torque and fuel conversion efficiency. Rinaldini et al. [17] also carried out experimental and numerical studies to analyse the influence of Miller cycle. The results showed that Miller cycle operation reduced NOx and soot emissions by 25% and 60% respectively, which was attained with a fuel efficiency penalty of 2% in a light-duty diesel vehicle in the European Driving Cycle. Experimental investigation by Garg et al. [18] showed that the cylinder throttling via early (EIVC) and late (LIVC) IVC reduced the volumetric efficiency. This resulted in a lower in-cylinder mass, leading to an increase in EGT. The use of iEGR can retain hot residuals from the previous cycle, which allows for the improvement in exhaust thermal management and reduction in unburned HC and CO emissions at low engine loads [19–21].

Other effective means for reducing NOx emissions is the introduction of cooled EGR to the Miller cycle operation, as reported in our previous works [15,22]. Moreover, Kim et al. [23] experimentally studied the combined use of Miller cycle with EGR in a single cylinder diesel engine operating at low engine loads. The NOx emissions were reduced from 10 g/kWh to approximately 1 g/kWh. Verschaeren et al. [24] revealed NOx reduction levels of more than 70% when using Miller cycle and EGR in a HD diesel engine. Experimental and simulation studies by Benajes et al. [25,26] showed that EIVC and EGR can decrease the combustion temperatures and create leaner local equivalence ratios, effectively curbing NOx and soot formation.

However, the lower in-cylinder air-fuel ratio resulted from the combined use of Miller cycle and EGR at high engine loads can deteriorate the combustion process, yielding poor fuel conversion efficiency and high levels of soot and CO emissions [27–30]. Therefore, higher intake air boost is necessary in order to increase or maintain the in-cylinder air-fuel ratio when both Miller cycle and EGR strategies are applied at high engine loads. Kovács et al. [29] studied the effect of boost pressure on Miller cycle operation with EGR in the upper load range of a HD diesel engine. A significant improvement in soot and CO emissions was achieved as well as a reasonable trade-off with NOx. Further investigations by Kovács et al. [31] demonstrated that a very high turbocharger efficiency is needed to minimise the fuel consumption of the

Miller cycle operation. Many other works have also shown that a higher boost pressure is the key enabler for Miller cycle operation with EGR to achieve simultaneous high fuel conversion efficiency and low exhaust emissions [32–34].

To address the challenges encountered by current HD diesel engines, research and development work is required in order to further optimise the combustion process. This study aims to investigate advanced VVA-based combustion control strategies as means to improve upon exhaust temperatures and reduce the emissions at low load operation as well as to increase fuel conversion efficiency and reduce total fluid consumption at high load operation.

In particular, the current work is the first attempt to experimentally study and analyse the potential of VVA-based technology at low and high engine load conditions. Advanced combustion control strategies including the combinations of Miller cycle, internal and external EGR, post injection, and highly boosted operation for emissions and EGT control and efficiency improvement were demonstrated accordingly. In the last section, an overall efficiency and emissions analysis based on the Euro VI NOx limit was carried out to determine the effectiveness of VVA-based strategies for lowering the total fluid consumption of a HD diesel engine.

The experimental study was carried out on a single-cylinder HD diesel engine equipped with a VVA system. A one-dimensional (1D) engine simulation model was used to calculate the mean in-cylinder gas temperatures (T_m). The effectiveness of Miller cycle with iEGR was examined at a light engine load of 2.2 bar IMEP (e.g. test point 1). The application of Miller cycle operation combined with cooled EGR and post injection was investigated at a part engine load of 6 bar IMEP (e.g. test point 2). Moreover, the potential of Miller cycle operating with EGR and a higher boost pressure was explored at a high engine load of 17 bar IMEP (e.g. test point 3). The overall engine efficiency and cost-benefit of the optimum VVA-based combustion control strategies were analysed and compared to those of the baseline diesel combustion operation.

2. Experimental setup

2.1 Engine specifications and experimental facilities

Figure 1 shows the schematic diagram of the single cylinder heavy-duty diesel engine. A Froude Hofmann AG150 eddy current dynamometer was coupled to absorb the engine power output. Table 1 outlines the base hardware specifications of the test engine. The combustion system was designed based on the Yuchai YC6K 6-cylinder diesel engine, which consisted of a 4-valve swirl-oriented cylinder head and a stepped-lip piston bowl design with a geometric compression ratio of 16.8. The bottom end/short block was AVL-designed with two counter-rotating balance shafts.

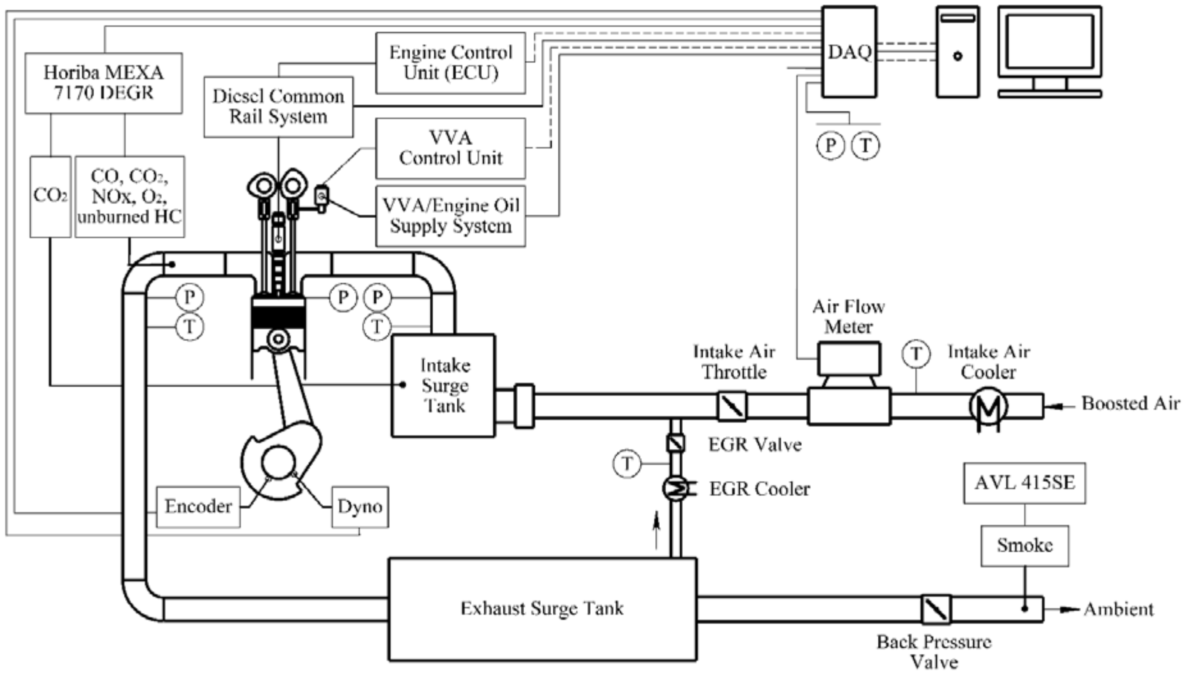

Figure 1. Layout of the engine experimental setup.

Table 1. Specifications of the test engine.

Displaced Volume	2026 cm^3
Stroke	155 mm
Bore	129 mm
Connecting Rod Length	256 mm
Geometric Compression Ratio	16.8
Number of Valves	4
Piston Type	Stepped-lip bowl
Diesel Injection System	Bosch common rail
Nozzle design	8 holes, 0.176 mm hole diameter, included spray angle of 150°
Maximum fuel injection pressure	2200 bar
Maximum in-cylinder pressure	180 bar

The compressed air was supplied by an AVL 515 sliding vanes supercharger with closed loop control. Two surge tanks were installed to damp out the strong pressure fluctuations in intake and exhaust manifolds. The intake manifold pressure was finely controlled by a throttle valve located upstream of the intake surge tank. An Endress+Hauser Proline t-mass 65F thermal mass flow meter was used to measure the fresh air mass flow rate. An electronically controlled butterfly valve located downstream of the exhaust surge tank was used to independently control the exhaust back pressure. High-pressure loop cooled external EGR was introduced to the engine intake manifold located between the intake surge tank and throttle by using a pulse width modulation-controlled EGR valve and the pressure differential between the intake and exhaust manifolds. Coolant and oil pumps were driven by separate electric motors. Water cooled heat exchangers were used to control the temperatures of the boosted intake air and external EGR as well as engine coolant and lubricating oil. The coolant and oil temperatures were kept within 356 ± 2 K. The oil pressure was maintained within 4.0 ± 0.1 bar throughout the experiments.

The fuel injection parameters such as the injection pressure, start of injection (SOI), and the number of injections (up to three injections per cycle) were controlled by a dedicated electronic control unit (ECU). During the experiments, the diesel fuel was injected into the engine by a high-pressure solenoid injector through a high pressure pump and a common rail with a maximum fuel pressure of 2200 bar. The fuel consumption was determined by measuring the total fuel supplied to and from the high pressure pump and diesel injector via two Coriolis flow meters. The specifications of the measurement equipment can be found in Appendix A.

2.2 Variable valve actuation system

The engine was equipped with a prototype hydraulic lost-motion VVA system, which incorporated a hydraulic collapsing tappet on the intake valve side of the rocker arm. The VVA system allowed for the adjustment of the IVC timing and thus enable Miller cycle operation. The intake valve opening (IVO) and closing (IVC) of the baseline case were set at 367 and -174 crank angle degrees (CAD) after top dead centre (ATDC), respectively. All valve events were considered at 1 mm valve lift and the maximum intake valve lift event was set to 14 mm.

In addition, this system enables a 2IVO event during the exhaust stroke in order to trap iEGR and increase the residual gas fraction. The earliest opening timing and the latest closing timing of the 2IVO strategy were set at 160 CAD ATDC and 230 CAD ATDC, respectively. The maximum valve lift of this configuration was 2 mm. Figure 2 shows the intake and exhaust valve profiles for the baseline engine operation as well as for the LIVC and 2IVO cases. The effective compression ratio, ECR, was calculated as

$$ECR = \frac{V_{ivc\_eff}}{V_{tdc}} \quad (1)$$

where V_{tdc} is the cylinder volume at top dead centre (TDC) position, and V_{ivc_eff} is the effective cylinder volume where the in-cylinder compressed air pressure is extrapolated to be identical to the intake manifold pressure [35,36].

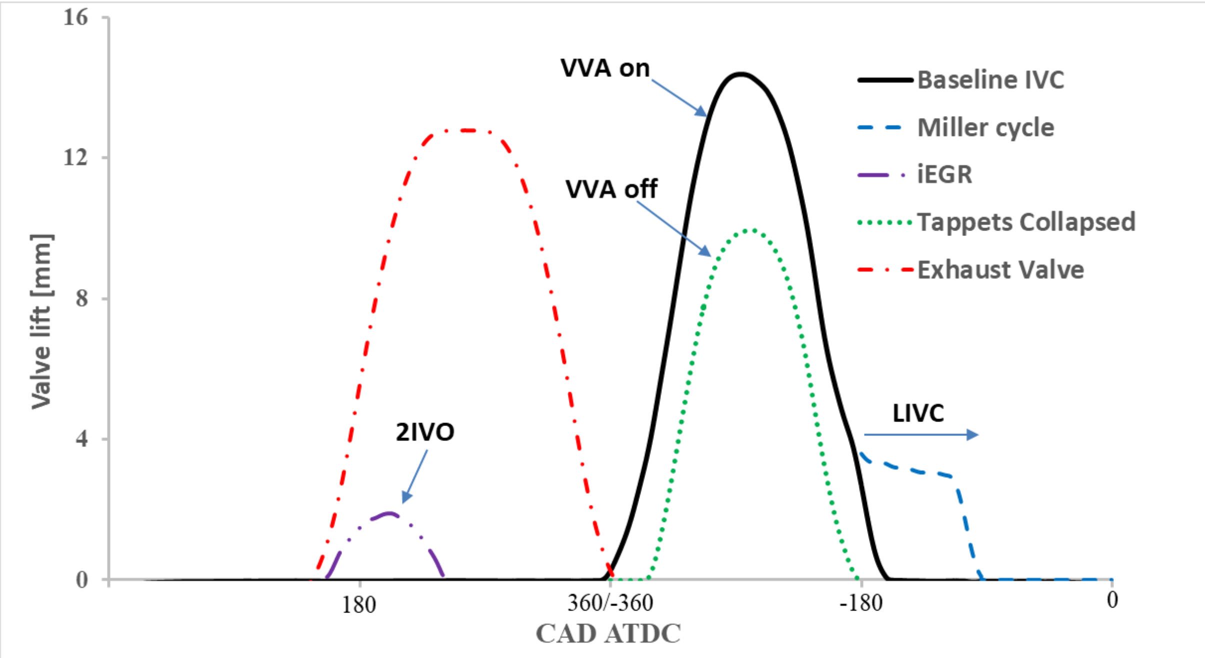

Figure 2. Fixed exhaust and variable intake valve lift profiles.

2.3 Exhaust emissions measurement

A Horiba MEXA-7170 DEGR emission analyser was used to measure the exhaust gases such as NOx, HC, CO, and CO_2 in the exhaust pipe before the exhaust back pressure valve. In this analyser system, gases including CO and CO_2 were measured through a non-dispersive infrared absorption (NDIR) analyser, HC was measured by a flame ionization detector (FID), and NOx was measured by a chemiluminescence detector (CLD). To allow for the measurement at elevated back pressure, a high pressure sampling module was used between the exhaust sampling point and the emission analyser. A heated line was deployed to maintain the exhaust gas sample temperature of approximately 192℃ to avoid condensation. The smoke number was measured downstream of the exhaust back pressure valve using an AVL 415SE Smoke Meter. The measurement was taken in filter smoke number (FSN) basis and thereafter was converted to mg/m^3 [37]. All the exhaust gas components were converted to net indicated specific gas emissions (in g/kWh) according to [38]. In this study, the EGR rate was defined as the ratio of the measured CO_2 concentration in the intake surge tank ($(CO_2\%)_{intake}$) to the CO_2 concentration in the exhaust manifold ($(CO_2\%)_{exhaust}$) as

$$EGR \text{ rate} = \frac{(CO_2\%)_{intake}}{(CO_2\%)_{exhaust}} \times 100\% \tag{2}$$

2.4 Data acquisition and analysis

The instantaneous in-cylinder pressure was measured by a Kistler 6125C piezo-electric pressure transducer with a sampling resolution of 0.25 CAD. The high speed and low speed National Instruments data acquisition (DAQ) cards were used to acquire the high and low frequency signals from the measurement devices. The captured data from the DAQ as well as the resulting engine parameters were displayed in real-time by an in-house developed transient combustion analysis software.

The crank angle based in-cylinder pressure traces were recorded through an AVL FI Piezo charge amplifier, averaged over 200 consecutive engine cycles, and used to calculate the IMEP and apparent heat release rate (HRR). According to [1], the apparent HRR was calculated as

$$HRR = \frac{\gamma}{(\gamma - 1)}\, p\, \frac{dV}{d\theta} + \frac{1}{(\gamma - 1)}\, V\, \frac{dp}{d\theta} \tag{3}$$

where γ is defined as the ratio of specific heats, which was assumed constant at 1.33 throughout the engine cycle [39]; V and p are the in-cylinder volume and pressure, respectively; and θ is the crank angle degree.

In this study, the mass fraction burned (MFB) was defined by the ratio of the integral of the HRR and the maximum cumulative heat release. Combustion phasing (CA50) was determined by the crank angle of 50% MFB. Combustion duration was represented by the period of time between the crank angles of 10% (CA10) and 90% (CA90) MFB. Ignition delay was defined as the period of time between the main SOI and the start of combustion (SOC), denoted as 0.3% MFB point of the average cycle. The in-cylinder combustion stability was monitored by the coefficient of variation of the IMEP (COV_IMEP) over the sampled cycles.

3. Methodology

3.1 Estimation of the total fluid consumption

An increase in engine-out NOx emissions can lead to a higher consumption of aqueous urea solution in the aftertreatment system of an SCR equipped HD diesel engine. This can adversely affect the total engine fluid consumption and thus the engine operational cost. Therefore, the total fluid consumption is estimated in this study in order to take into account both the measured diesel flow rate ($\dot{m}_{diesel}$) and the estimated urea consumption in the SCR system ($\dot{m}_{urea}$). As the relative prices between diesel fuel and urea are different in different countries and regions, the price and property of urea is simulated to be the same as diesel fuel in this study [40,41]. According to [40,42], the required aqueous urea solution to meet the Euro VI NOx limit of 0.4 g/kWh can be estimated as 1% of the diesel equivalent fuel flow per g/kWh of NOx reduction.

$$\dot{m}_{urea} = 0.01\left(NOx_{engine-out} - NOx_{Euro\ VI}\right)\dot{m}_{diesel} \tag{5}$$

By adding the measured diesel flow rate to the estimated urea flow rate allowed for the calculation of total fluid consumption, which was defined as

$$\dot{m}_{total} = \dot{m}_{diesel} + \dot{m}_{urea} \tag{6}$$

3.2 Calculation of the mean in-cylinder gas temperature

In order to better analyse the influence of different combustion control strategies on in-cylinder combustion process, a 1D engine simulation has been carried out using Ricardo Wave software to estimate the mean in-cylinder gas temperatures. As demonstrated in our previous works [22,43], the combustion process was simulated by using the experimentally derived HRR profile based on the measured in-cylinder pressure, the heat transfer was calculated by the Woschni heat transfer model, and the thermodynamic state of the in-cylinder gas was estimated by using a two-zone model. In all cases, the intake air mass flow rate, IMEP, in-cylinder pressure, intake and exhaust manifold pressures were calibrated against the experimental data in order to validate the 1D engine model. Finally, the validated 1D engine model was used to calculate the mean in-cylinder gas temperatures.

3.3 Test conditions

In this study, the experimental work was carried out at a speed of 1150 rpm and a light engine load of 2.2 bar IMEP, as well as at a constant speed of 1250 rpm and the engine loads of 6 bar and 17 bar IMEP. These conditions were denoted as test point 1, 2, and 3, respectively. Figure 3 shows the location of the World Harmonized Stationary Cycle (WHSC) test points over a heavy-duty diesel engine operation map. The WHSC is a legislated test cycle adopted in the Euro VI emission standard [44]. The size of the circle represents the weighting factor. A larger circle indicates a higher relative weight of the engine operation condition over the WHSC. Figure 3 also shows the three test points, which are located within the area of the WHSC test cycle. In particular, the test point 1 represents a typical engine operating condition of a transient HD drive cycle and is typically characterised by an exhaust gas temperature below 200°C.

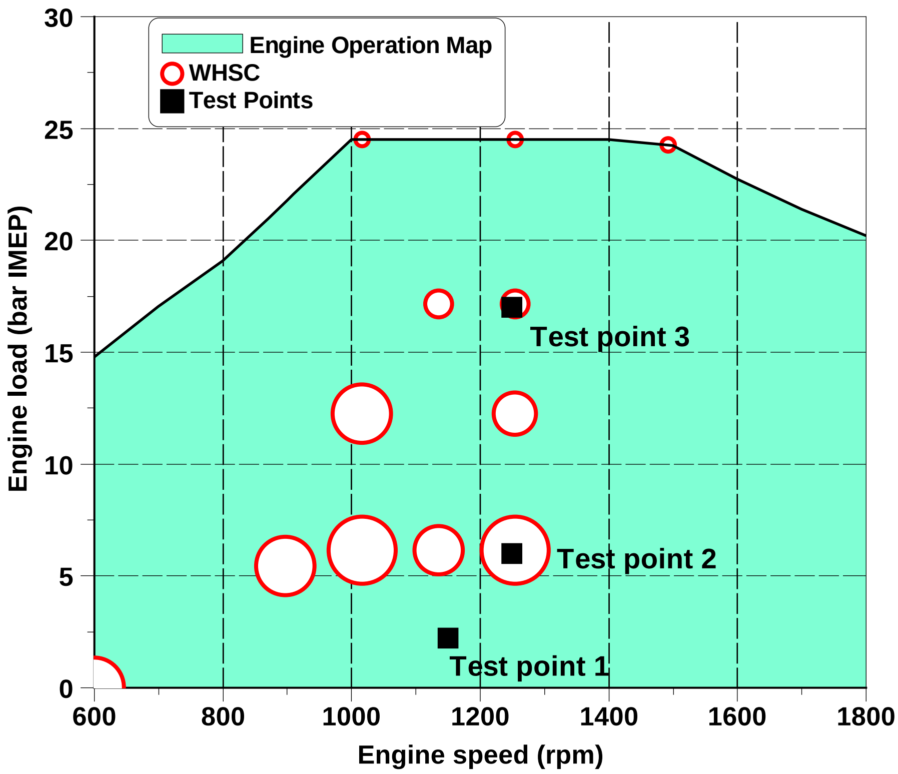

Figure 3. Experimental test points and WHSC operating conditions over an estimated HD diesel engine speed-load map.

Table 2 summarises the engine test conditions for the different engine combustion control strategies used at the three test points. The intake pressure set points of the baseline engine operation were taken from a corresponding 6-cylinder HD diesel engine, which complies with the Euro V emissions legislation. The IVC in the Miller cycle mode was set at -100 and -105 CAD ATDC at the low engine loads of 2.2 bar IMEP (test point 1) and 6 bar IMEP (test point 2), respectively. These settings have been determined in our previous studies [15,43]. At the high load of 17 bar IMEP (test point 3), the IVC was advanced to -115 CAD ATDC. Such settings were necessary in order to avoid combustion instability, excessive smoke emissions, as well as to minimise the demand on the boosting system when operating the engine with Miller cycle and EGR.

At the test point 1, the optimum operation mode was determined when the EGT achieved more than 200°C necessary to initiate the emissions control operation while achieving comparable emissions and efficiency to the baseline operation. This was fulfilled by the addition of iEGR via 2IVO event to a Miller cycle mode with an IVC at -100 CAD ATDC. The diesel injection timing and the fuel injection pressure were held constant at -5.7 CAD ATDC and 500 bar, respectively. The exhaust back pressure was kept similar to the intake pressure for all three operating modes at this test point.

At the test point 2, the optimum operating condition employed an external EGR of 15% combined with a Miller cycle operation (LIVC at -105 CAD ATDC). In addition, a 12 mm^3 post injection at 18 CAD ATDC was applied. This post injection strategy was found to give the best trade-off between exhaust emissions and fuel conversion efficiency in our previous study [43]. Furthermore, a small pilot injection of 3 mm^3 with a constant dwell time of 1 ms prior to the main injection timing was employed in order to keep the maximum pressure rise rate (PRR) below 20 bar/CAD.

At the test point 3, the optimum operation mode used an EGR rate of 15% and a higher intake pressure of 2.62 bar. The exhaust back pressure was adjusted to maintain a constant pressure differential of 0.10 bar above the intake pressure, simulating the real engine operation with a turbocharger and achieving the required EGR rate. The fuel injection timings of three operating modes were optimised between -2.5 and -12 CAD ATDC in order to achieve the minimum total fluid consumption.

Diesel injection pressures were increased at higher engine loads in order to control the levels of smoke but held constant at a given load as shown in Table 2. The maximum in-cylinder pressure was limited to 180 bar. Stable engine operation was determined by controlling the COV_IMEP below 3%.

Table 2 Engine testing conditions for baseline, Miller cycle, and optimum engine operations.

<table>
<tr><th>Test point</th><th>Engine speed</th><th>Engine load</th><th>Operating mode</th><th>Main SOI</th><th>Injection pressure</th><th>Intake pressure</th><th>Exhaust pressure</th><th>IVC</th><th>iEGR</th><th>eEGR</th><th>Pre-inj.</th><th>Post-inj.</th></tr>
<tr><td>-</td><td>rpm</td><td>bar IMEP</td><td>-</td><td>CAD ATDC</td><td>bar</td><td>bar</td><td>bar</td><td>CAD ATDC</td><td>-</td><td>%</td><td>-</td><td>-</td></tr>
<tr><td rowspan="3">1</td><td rowspan="3">1150</td><td rowspan="3">2.2</td><td>Baseline</td><td rowspan="3">-5.7</td><td rowspan="3">500</td><td rowspan="3">1.16</td><td rowspan="3">1.20</td><td>-178</td><td>No</td><td rowspan="3">0</td><td rowspan="3">No</td><td rowspan="3">No</td></tr>
<tr><td>Miller cycle</td><td>-100</td><td>No</td></tr>
<tr><td>Optimum</td><td>-100</td><td>Yes</td></tr>
<tr><td rowspan="3">2</td><td rowspan="3">1250</td><td rowspan="3">6.0</td><td>Baseline</td><td rowspan="3">-4</td><td rowspan="3">1150</td><td rowspan="3">1.44</td><td rowspan="3">1.54</td><td>-178</td><td rowspan="3">No</td><td>0</td><td rowspan="3">Yes</td><td>No</td></tr>
<tr><td>Miller cycle</td><td>-105</td><td>0</td><td>No</td></tr>
<tr><td>Optimum</td><td>-105</td><td>15</td><td>Yes</td></tr>
<tr><td rowspan="3">3</td><td rowspan="3">1250</td><td rowspan="3">17.0</td><td>Baseline</td><td>-6</td><td rowspan="3">1450</td><td>2.32</td><td>2.42</td><td>-178</td><td rowspan="3">No</td><td>0</td><td rowspan="3">No</td><td rowspan="3">No</td></tr>
<tr><td>Miller cycle</td><td>-7.5</td><td>2.32</td><td>2.42</td><td>-115</td><td>0</td></tr>
<tr><td>Optimum</td><td>-8</td><td>2.62</td><td>2.72</td><td>-115</td><td>15</td></tr>
</table>

4. Results and discussions

4.1 Analysis of the in-cylinder pressure and heat release rate

Figures 4, 5, and 6 show a comparison of the in-cylinder pressure and heat release rate (HRR) for the baseline, Miller cycle, and optimum engine operations at the three test points. At the test point 1 shown in Figure 4, the Miller cycle and the optimum cases were characterised by significantly lower in-cylinder gas pressure than that of the baseline operation. This was attributed to a later initiation of the compression process resulted from the LIVC (e.g. lower ECR), which lowered the in-cylinder gas pressure and temperature [45]. Consequently, the combustion process was shifted far away from TDC. Despite the recirculation of residual gases back to the cylinder could lead to a higher specific heat capacity, the introduction of iEGR on the optimum engine operating condition enhanced the combustion process via a higher in-cylinder gas temperature resulted from the trapped hot residual gas [15]. This was a reason for a relatively more advanced SOC and higher peak HRR than the Miller cycle operation, which can potentially improve the combustion efficiency and fuel conversion efficiency.

At the test point 2, the optimised main SOI of the three different operating modes was obtained at -4 CAD ATDC, as depicted in Figure 5. The application of an LIVC in the Miller cycle and optimum operation modes reduced the in-cylinder pressure during the compression stroke as a result of a lower ECR. In the optimum engine operation mode, the combined use of a post injection and EGR lowered the peak HRR and further decreased the maximum in-cylinder gas pressure. This was attributed to a decrease in the amount of fuel injected during the main injection combined with the dilution and specific heat capacity effects of the EGR that slow down the reaction rates [46]. A second heat release peak was generated by the combustion of the post injected fuel, which can help to minimise soot emissions by enhancing fuel-air mixing and increasing the combustion temperature of late combustion process, according to the findings of [47,48].

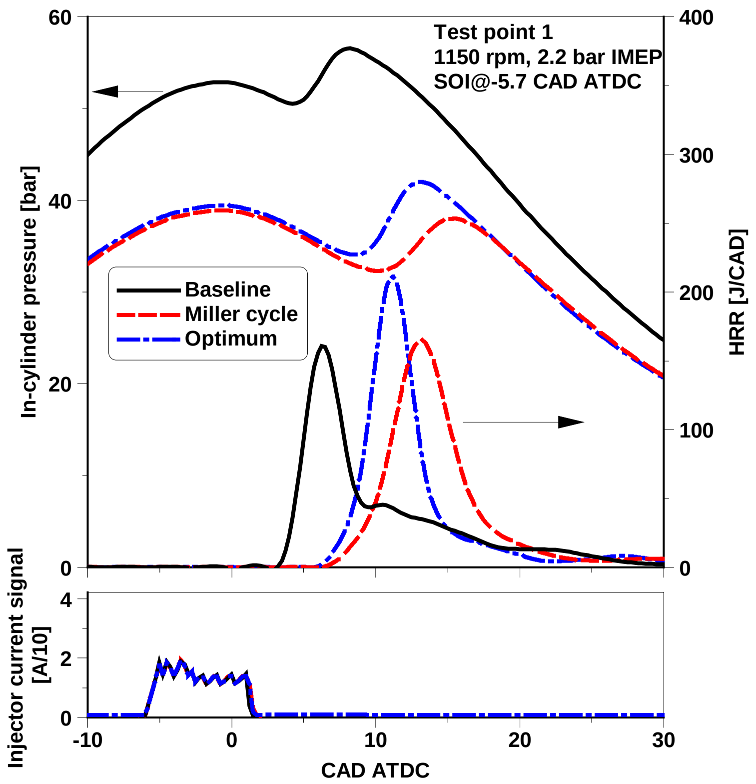

Figure 4. In-cylinder pressure, HRR, and diesel injector signal for different engine combustion control strategies at test point 1.

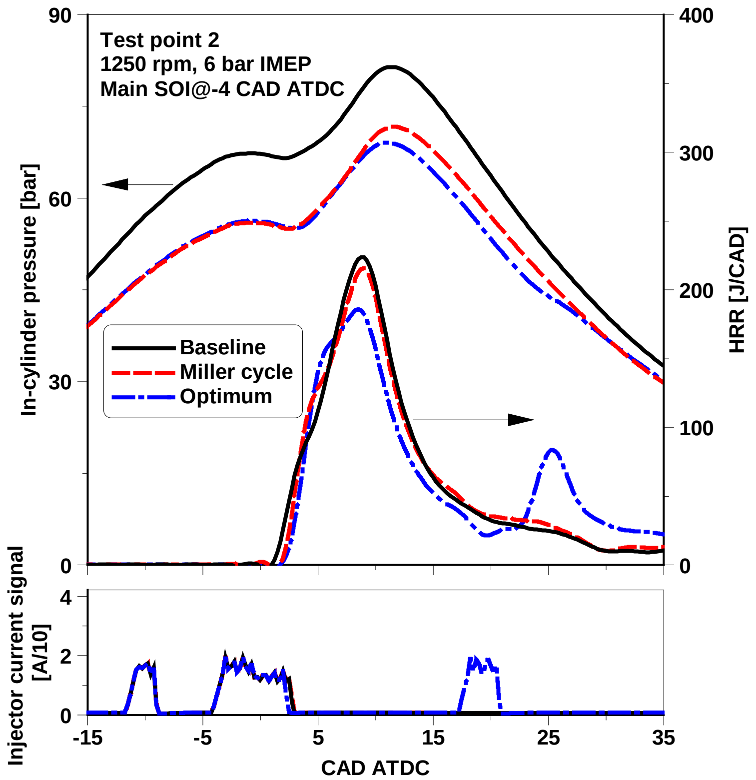

Figure 5. In-cylinder pressure, HRR, and diesel injector signal for different engine combustion control strategies at test point 2.

As the engine load was increased to 17 bar IMEP, the diesel injection timing was optimised to achieve the minimum total fluid consumption. The Miller cycle operation allowed for a more advanced SOI than the baseline engine operation, as shown in Figure 6. However, the level of NOx reduction achieved with a Miller cycle strategy was limited primarily due to the small impact on the in-cylinder flame temperature, as reported by Benajes et al. [49].

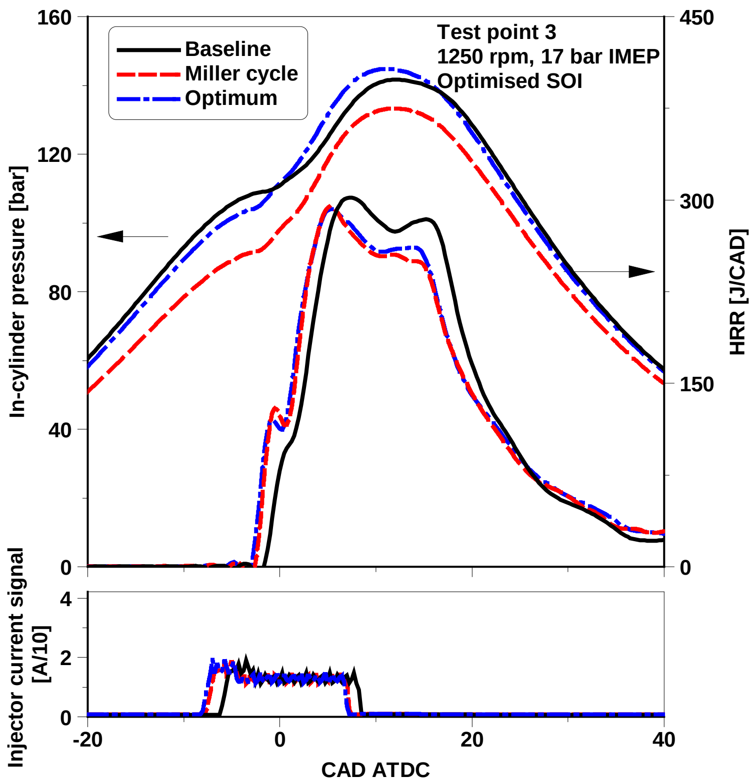

Figure 6. In-cylinder pressure, HRR, and diesel injector signal for different engine combustion control strategies at test point 3.

The use of EGR can effectively curb NOx emissions but the fuel conversion efficiency could be compromised when introducing EGR to Miller cycle operation at high engine loads. This is because of a decrease in the charging efficiency and a reduction of the lambda when using the LIVC strategy, according to the findings of [17]. In order to overcome such shortcomings, higher boost pressure was adopted in the optimum engine operation mode to improve the in-cylinder air-fuel ratio. This helped to increase the compression pressure while maintaining the potential benefit of a more advanced combustion process for maximum fuel conversion efficiency and minimum NOx emissions.

It should be noted that a conventional turbocharging system is likely not able to deliver the required air flow rate when operating the engine with Miller cycle and EGR [50]. For this reason, a more sophisticated boosting system such as a two-stage variable geometry turbocharger configuration would be needed to deliver the desired boost pressures and overcome this limitation of a Miller cycle engine operation [31,51,52]. However, a high-performance turbocharging system would require additional cost, thus increasing the total engine operational cost [2,52,53].

Figure 7 shows the calculated mean in-cylinder gas temperatures of different engine combustion control strategies at the three test points. The use of Miller cycle strategy via an LIVC decreased the gas temperatures during the compression stroke, especially at the test point 1 due to the use of a relatively later IVC timing than that employed in the other two test points. The reduced compressed gas temperatures were attributed to a decrease in the ECR. However, the peak mean in-cylinder gas temperature was increased when compared to the baseline engine operation. This happened because of a reduction in the intake air mass flow rate, which decreased the in-cylinder heat capacity during the combustion event [25].

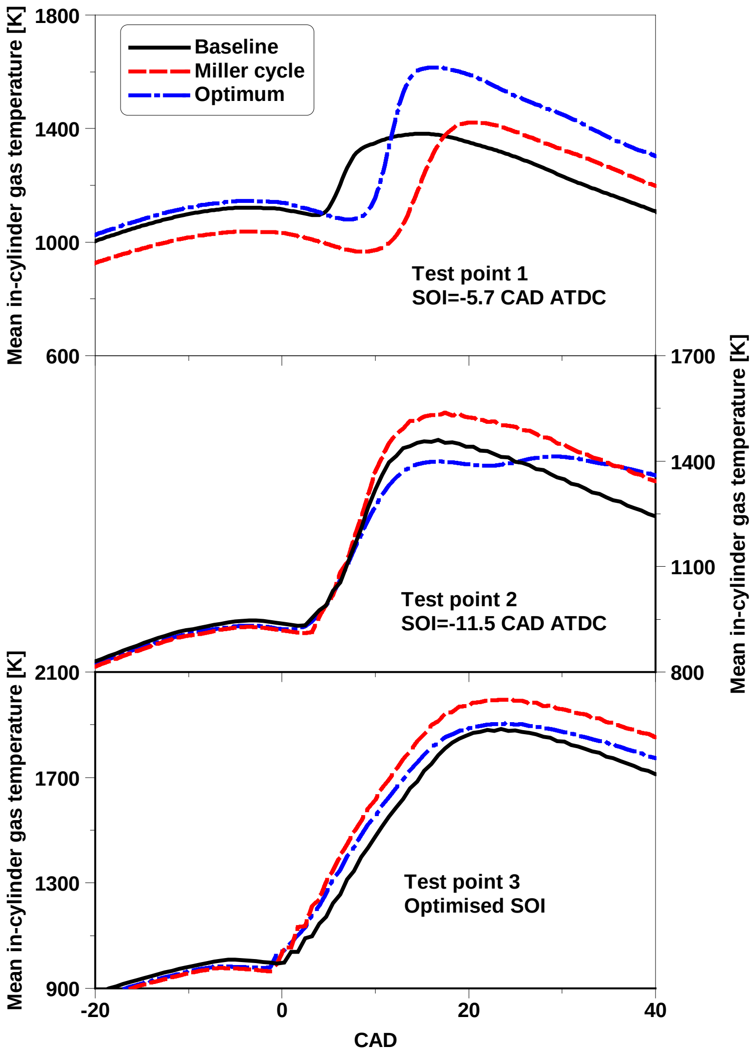

Figure 7. Calculated mean in-cylinder gas temperatures for baseline, Miller cycle, and optimum engine operations at the three test points.

The addition of iEGR to the Miller cycle operation at the test point 1 increased the compressed gas temperature owing to the presence of hot residual gas, despite the higher heat capacity of the in-cylinder charge. This resulted in a higher peak T_m than the Miller cycle case as well as higher temperatures during the expansion stroke. At the test point 2, the introduction of EGR in the optimum operation mode had little impact on the compressed gas temperature. The post injection, however, led to a reduction in the peak combustion temperature and an increase in the mean in-cylinder gas temperatures during the late stages of the combustion process, which can help to raise the EGT and improve the SCR operation. At the test point 3, the optimum mode with the use of a higher intake pressure and EGR increased the T_m during the combustion process compared to the baseline engine operation, despite a reduction in the T_m during the compression stroke. This was a result of the more advanced SOI, which led to earlier and faster heat release than that of the baseline operation.

4.2 Combustion characteristics

Figure 8 shows the resulting heat release characteristics for the different engine combustion control strategies at the three test points. At the test point 1, the use of an LIVC had a significant impact on the ignition delay, increasing the ignition delay by approximately 4 CAD compared to the baseline operation. This was a result of the reduced ECR, which delayed the SOC. This was also the reason for the delayed combustion phasing (CA50). However, a higher degree of premixed combustion accelerated the combustion rate of the late combustion phase as represented by a shorter period of CA50-CA90. As a result, a shorter combustion duration was obtained than that of the baseline operation. At the test points 2 and 3, however, the Miller cycle operation had less impact on the ignition delay compared to that of the test point 1. This could be explained by the use of a relatively earlier IVC timing and a better ignition condition when operating at a relatively higher engine load. The later ignition and longer combustion process for the Miller cycle cases lengthened the late combustion phase as shown by the longer CA50-CA90 period. These effects contributed to a longer combustion duration (CA10-CA90).

In comparison to the Miller cycle operation, the use of iEGR on the optimum operation mode advanced the SOC and thus decreased the ignition delay at test point 1. This combustion strategy also advanced the CA50 and led to a shorter combustion duration despite the slightly longer period of CA50-CA90. At the test point 2, the addition of a post injection delayed the CA50 as more diesel fuel was burned during a relatively later combustion phase. In addition, the introduction of EGR in the optimum operation mode contributed to the resulting later CA50 as the lower oxygen concentration decreased the combustion rate. As a result, the period of

CA50-CA90 was longer for the optimum engine operation with post injection and EGR. These effects resulted in an increase in the combustion duration by up to 5.5 CAD when compared to the Miller cycle operation. At the test point 3, the Miller cycle mode allowed for a more advanced SOI to achieve the minimum total fluid consumption, resulting in a slightly earlier CA50 than the baseline engine operation. In the optimum engine operation, the use of EGR and a higher boost pressure resulted in similar heat release characteristics to that of the Miller cycle operation.

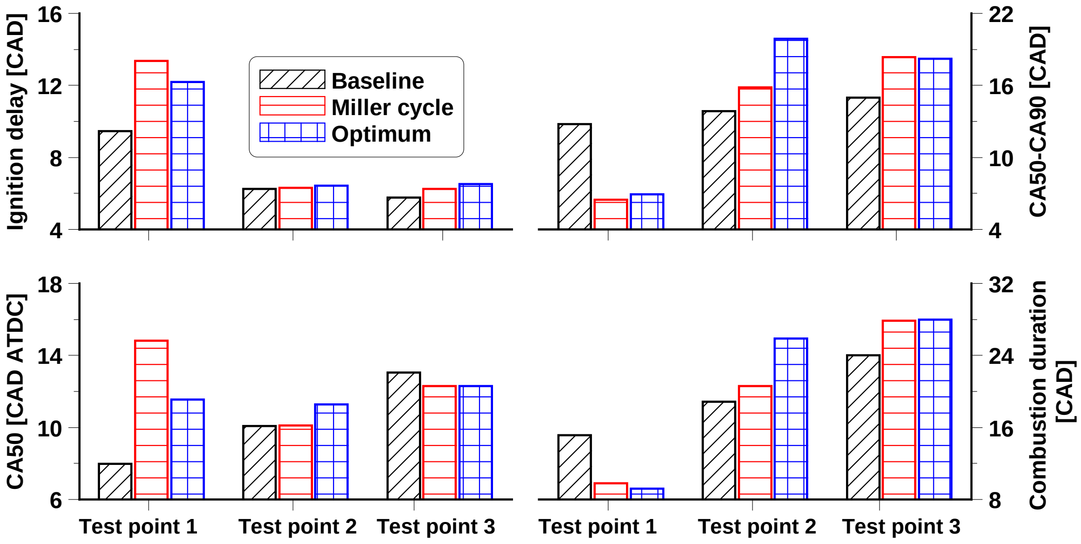

Figure 8. Heat release characteristics for baseline, Miller cycle, and optimum engine combustion control strategies at the three different test points.

4.3 Engine-out emissions

Figure 9 depicts the engine-out emissions for the baseline, Miller cycle, and optimum engine operations at the three different test points. At the test point 1, the engine-out NOx emissions were reduced slightly in the Miller cycle operation due to the decreased mass of air and the lower burned gas temperature caused by the LIVC strategy [43]. However, the NOx emissions were increased slightly by the addition of iEGR. This was attributed to the introduction of hot residual gas, which shortened the combustion duration and increased the combustion temperature. Nevertheless, the use of an LIVC, with and without adding iEGR, significantly decreased soot emissions from approximately 0.05 g/kWh in the baseline operation to less than 0.01 g/kWh in the Miller cycle operation. This can be explained by the higher degree of premixed combustion resulted from the longer ignition delay, which improved the air-fuel mixing and consequently the combustion process. In addition, the resulting higher combustion temperature helped to improve the oxidation of smoke, which contributed to the reduction in soot emissions. The longer ignition delay and the later combustion process, however, resulted in higher levels of unburned HC and CO emissions. Nevertheless, the introduction of iEGR helped to curb the formation of HC and CO as the trapped hot residual gas shortened the ignition delay, increased the combustion temperature, and consequently improved the combustion process.

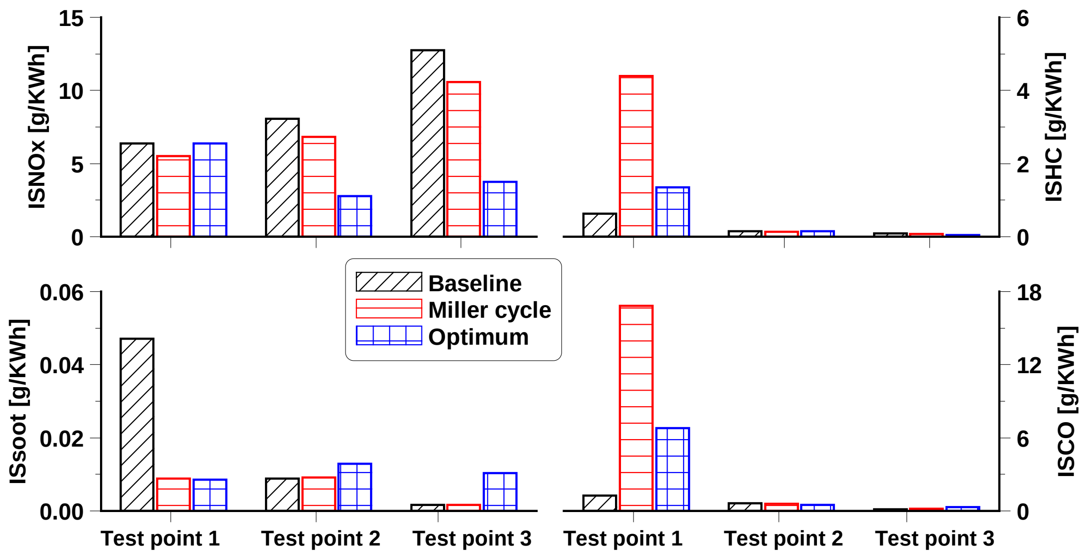

Figure 9. Exhaust emissions for baseline, Miller cycle, and optimum engine combustion control strategies at the three different test points.

For both test points 2 and 3, the Miller cycle operation achieved slightly lower engine-out NOx emissions than the baseline cases. A significant reduction in NOx emissions was obtained via the addition of EGR owing to the lower combustion temperature and lower in-cylinder oxygen concentration. However, the in-cylinder oxygen availability of the combined use of Miller cycle and EGR can be decreased noticeably, resulting in excessive smoke and CO emissions, as demonstrated by Verschaeren et al. [24]. Therefore, an advanced combustion control strategy was employed to help address these issues. As showed in Figure 9, the use of a post injection at the test point 2 and a highly boosted strategy at the test point 3 helped to curb the levels of soot emissions to approximately 0.01 g/kWh. All engine combustion control strategies at the test points 2 and 3 yielded significantly lower levels of CO and unburned HC than those of the test point 1. This was primarily because of the higher gas temperatures during the expansion and exhaust strokes as the engine load increased.

4.4 Engine performance

Figure 10 depicts the engine performance parameters for the baseline, Miller cycle, and optimum engine operations at the three different test points. The LIVC strategy in the Miller cycle operation reduced the lambda due to a reduction of the in-cylinder mass trapped when compared to the baseline cases. This was the primary reason for an increase in EGT from 163℃ in the baseline operation to 203℃ in the optimum operation, which is extremely important for achieving efficient exhaust aftertreatment operation at low engine loads. The delayed combustion process and longer combustion duration for the Miller cycle operation adversely affected the fuel conversion efficiency. In particular, the lower combustion efficiency of 96.1% at the test point 1 contributed to a decrease in the fuel conversion efficiency of 5% to 38.9%. This was a result of an increase in unburned HC and CO emissions caused by the lower combustion temperatures.

Compared to the Miller cycle case, the addition of iEGR increased the combustion efficiency from 96.1% to 98.6% and the fuel conversion efficiency from 38.9% to 40.4% while operating the engine at the test point 1. This was attributed to the presence of hot residual gas, which helped improve the combustion process and resulted in a higher lambda value. At the test point 2, the optimum engine operation with post injection and EGR decreased the lambda further, yielding a higher EGT. These effects combined with a longer combustion duration resulted in a reduction in fuel conversion efficiency when comparing to both baseline and Miller cycle operations. However, the lambda of the optimum engine operation at test point 3 was maintained the same to the Miller cycle operation via a higher intake pressure. The highly boosted strategy together with a more advanced combustion phasing in the optimum engine operation led to an increase in the fuel conversion efficiency of 3.3% to 46.5% compared to the Miller cycle mode. This was more than the fuel conversion efficiency produced by baseline case.

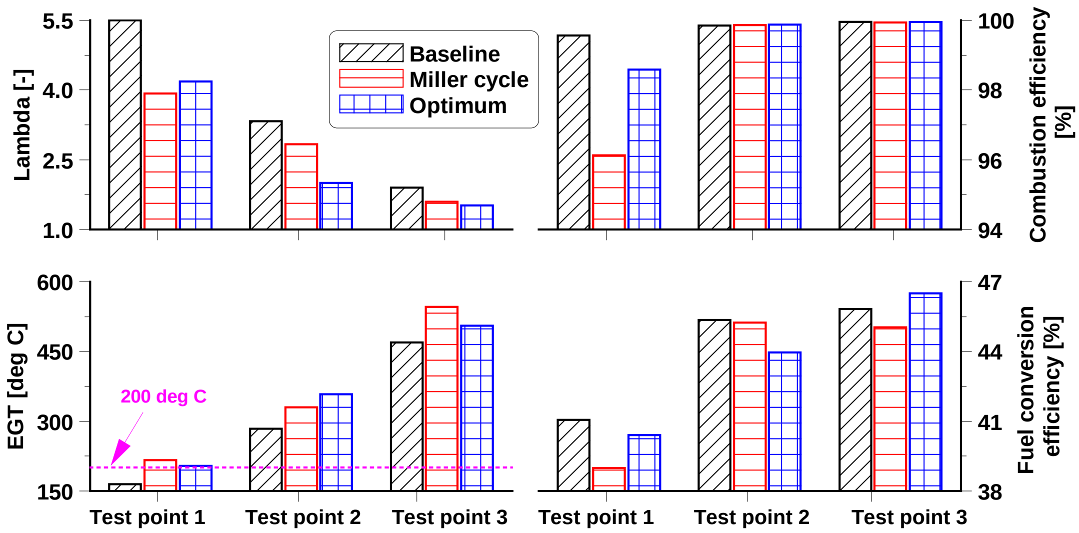

Figure 10. Engine performance for baseline, Miller cycle, and optimum engine combustion control strategies at the three different test points.

4.5 Overall engine efficiency and potential benefit analysis

In this section, the overall engine efficiency of different engine combustion control strategies was analysed by taking into account the consumption of aqueous urea solution in the SCR system. Additionally, the potential benefit of advanced VVA-based combustion control strategies was demonstrated by comparing the results of the optimum cases to those of the baseline engine operation.

The estimated urea flow rate in the aftertreatment system and the resulting total fluid consumption are depicted in Figure 11. As the urea consumption depends mainly on engine-out NOx emissions, reductions in the levels of engine-out NOx can help minimise the use of urea in the SCR system. The Miller cycle and the optimum engine operations decreased the urea consumption via lower engine-out NOx emissions. This helped to minimise the total fluid consumption, particularly at high engine load (e.g. test point 3) where the total fluid consumption was reduced from 7.35 kg/h in the baseline case to 6.95 kg/h in the optimum engine operation mode. At the test point 1, however, the Miller cycle and optimum engine operations led to a slight increase in total fluid consumption when compared to the baseline operation. This was attributed to the lower fuel conversion efficiency and similar level of engine-out NOx emissions.

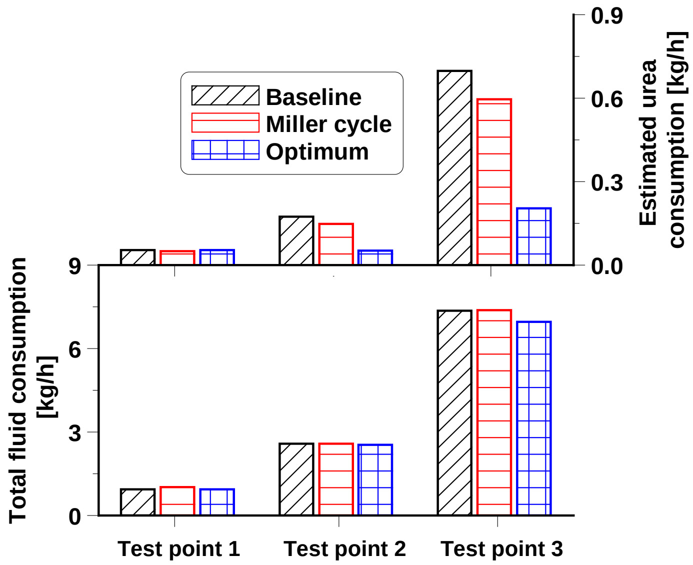

Figure 11. Overall engine efficiency analysis for baseline, Miller cycle, and optimum engine operation at the three different test points.

Figure 12 provides an overall assessment of the potential benefit of the VVA-based optimum engine operation in terms of exhaust emissions, engine performance, and total fluid consumption at the three test points investigated. Positive results achieved in the optimum engine operation are denoted with a green circle while the negative results are highlighted with a red circle.

The results of the optimum engine operations were compared to the baseline cases. The analysis revealed that the Miller cycle operation with iEGR increased EGT by 40°C and minimised soot emissions by 82% at the test point 1. These improvements were attained at the expense of little variation in NOx emissions and a reduction of 1.5% on the fuel conversion efficiency, resulting in an increase in the total fluid consumption of 0.2%.

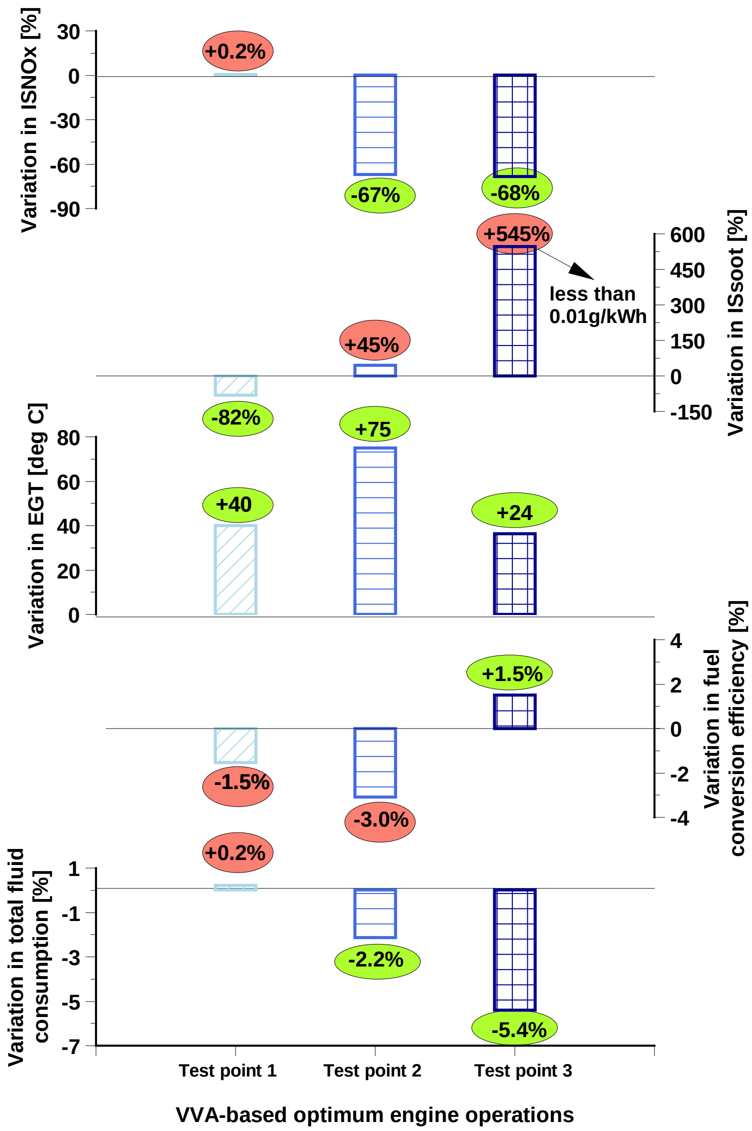

Figure 12. Overall evaluation of the potential benefit for the optimum engine operations at the three different test points. The variations in engine performance and emissions are relative to those for the baseline cases.

The combined use of Miller cycle with EGR and post injection increased the EGT by 75°C while reducing the NOx emissions by 67% at the test point 2. As a result, this strategy decreased the total fluid consumption by 2.2% despite the lower fuel conversion efficiency. At the test point 3, the combination of a Miller cycle strategy with EGR and a higher boost pressure increased the fuel conversion efficiency by 1.5% while reducing the NOx emissions by 68%. These improvements yield a reduction of 5.4% in the total fluid consumption. Overall, the results demonstrated that an advanced VVA-based combustion control strategy enables exhaust thermal management and exhaust emissions control of a HD diesel engine operating at low engine loads (e.g. test points 1 and 2). The findings also indicated that an alternative combustion control strategy with Miller cycle can attain higher fuel conversion efficiency and lower total fluid consumption than those typically found on a conventional HD diesel engine operating at high engine loads (e.g. test point 3).

5. Conclusions

In this study, experiments were performed on a HD diesel engine operating at a typical light engine load of 2.2 bar IMEP with low EGT and two other engine loads of 6 and 17 bar IMEP located within WHSC test cycle. The aim of the research was to investigate advanced VVA-based combustion control strategies as means to overcome the challenges encountered by current HD diesel engines. At 2.2 and 6 bar IMEP, the study was focused on increasing exhaust gas temperature for optimum exhaust emissions control. At 17 bar IMEP, the investigation aimed at increasing the fuel conversion efficiency and reducing the total fluid consumption. Both Miller cycle and iEGR operations were realised by means of a VVA system. Cooled external EGR and multiple injections were achieved via a high pressure loop EGR and a common rail fuel injection system, respectively. The primary findings can be summarised as follows:

1. Optimised VVA-based combustion control strategies were effective means of managing the exhaust gas temperature at low engine loads, increasing EGT by 40°C at 2.2 bar IMEP and by 75°C at 6 bar IMEP. In particular, the resulting EGT was higher than 200°C at 2.2 bar IMEP, which is more than the minimum necessary to initiate the exhaust emissions control. These improvements were attained at the expense of a slightly lower fuel conversion efficiency.
2. At a light engine load of 2.2 bar IMEP (test point 1), the Miller cycle strategy decreased soot emissions by 82% compared to the baseline engine operation. The addition of iEGR helped to improve the combustion efficiency via lower unburned HC and CO emissions.
3. At the part load of 6 bar IMEP (test point 2), the combination of Miller cycle with EGR and a post injection of 12 mm^3 at 18 CAD ATDC allowed for a reduction of 67% in NOx

emissions. Furthermore, the total fluid consumption was reduced by 2.2% despite a reduction in fuel conversion efficiency of 3.0%.

4. At the high load condition of 17 bar IMEP (test point 3), the optimum engine operation employed Miller cycle, EGR, and a higher boost pressure. This enabled an increase of 1.5% in fuel conversion efficiency and a reduction of 68% in NOx emissions. These improvements contributed to a reduction in total fluid consumption of 5.4%.
5. Overall, an advanced VVA-based combustion control strategy enabled exhaust emissions and EGT control at low engine loads, as well as helped to increase the fuel conversion efficiency for lower total fluid consumption at high engine loads. These improvements can minimise the total engine operational cost of future HD diesel engines.

Contact information

Wei Guan
Wei.guan@brunel.ac.uk
gwei916@163.com
Centre for Advanced Powertrain and Fuels Research
College of Engineering, Design and Physical Sciences
Brunel University London
Kingston Lane
Uxbridge
Middlesex UB8 3PH
United Kingdom

Acknowledgments

The first author, Mr W Guan, would like to acknowledge the Guangxi Yuchai Machinery Company for supporting his PhD study supervised by Prof. Zhao at Brunel University London.

Declaration of conflicting interests

The author(s) declared no potential conflicts of interest with respect to the research, authorship, and/or publication of this article.

Funding

The author(s) disclosed receipt of the following financial support for the research, authorship, and/or publication of this article: Funding for this project was provided by Guangxi Yuchai Machinery Company.

Definitions/Abbreviations

ATS	Aftertreatment System.

ATDC	After Firing Top Dead Center.
CA90	Crank Angle of 90% Cumulative Heat Release.
CA50	Crank Angle of 50% Cumulative Heat Release.
CA10	Crank Angle of 10% Cumulative Heat Release.
CAD	Crank Angle Degree.
CLD	Chemiluminescence Detector.
CO	Carbon Monoxide.
CO_2	Carbon Dioxide.
COV_IMEP	Coefficient of Variation of IMEP.
$(CO_2\%)_{intake}$	CO_2 concentration in the intake manifold.
$(CO_2\%)_{exhaust}$	CO_2 concentration in the exhaust manifold.
DAQ	Data Acquisition.
DOC	Diesel Oxidation Catalyst.
ECR	Effective Compression Ratio.
ECU	Electronic Control Unit.
EGR	Exhaust Gas Recirculation.
EGT	Exhaust Gas Temperature.
EVO	Exhaust Valve Opening.
EVC	Exhaust Valve Closing.
EIVC	Early Intake Valve Closing.
FID	Flame Ionization Detector.
FSN	Filter Smoke Number.
HCCI	Homogenous Charge Compression Ignition.
HRR	Heat Release Rate.
HC	Hydrocarbons.
HD	Heavy Duty.
iEGR	Internal Exhaust Gas Recirculation.
IMEP	Indicated Mean Effective Pressure.
IVO	Intake Valve Opening.
IVC	Intake Valve Closing.
ISsoot	Net Indicated Specific Emissions of Soot.
ISNOx	Net Indicated Specific Emissions of NOx.
ISCO	Net Indicated Specific Emissions of CO.

ISHC	Net Indicated Specific Emissions of Unburned HC.
LIVC	Late Intake Valve Closing.
LTC	Low Temperature Combustion.
MFB	Mass Fraction Burned.
$\dot{m}_{urea}$	Aqueous Urea Solution Consumption.
$\dot{m}_{diesel}$	Diesel Flow Rate.
$\dot{m}_{total}$	Total Fluid Consumption.
NDIR	Non-Dispersive Infrared Absorption.
NOx	Nitrogen Oxides.
PM	Particulate Matter
PCCI	Premixed Charge Compression Ignition.
PPCI	Partially Premixed Charge Compression Ignition.
PRR	Pressure Rise Rate.
SCR	Selective Catalytic Reduction.
SOI	Start of Injection.
SOC	Start of Combustion.
TDC	Firing Top Dead Centre.
Tm	Mean in-cylinder gas temperature.
VVA	Variable Valve Actuation.
WHSC	World Harmonized Stationary Cycle.

References

1. Heywood J.B, “Internal Combustion Engine Fundamentals,” ISBN 007028637X, 1988.
2. Posada, F., Chambliss, S., and Blumberg, K., “Costs of emission reduction technologies for heavy-duty diesel vehicles,” (February), 2016.
3. Federal legislation, “Final Rule for Greenhouse Gas Emissions and Fuel Efficiency Standards for Medium- and Heavy-Duty Engines and Vehicles - Phase 2,” 2016.
4. “California Air Resources Board, Final Report: Evaluating Technologies and Methods to Lower Nitrogen Oxide Emissions from Heavy-Duty Vehicles,” 2017.
5. Barbosa, F.C., “Heavy Duty Emission Standards Assessment - An Engine and Aftertreatment Technological Approach,” *SAE Tech. Pap.*, 2016, doi:10.4271/2016-36-

0167.

6. Bendu, H. and Murugan, S., "Homogeneous charge compression ignition (HCCI) combustion: Mixture preparation and control strategies in diesel engines," *Renew. Sustain. Energy Rev.* 38:732–746, 2014, doi:10.1016/j.rser.2014.07.019.

7. Shi, L., Zhang, L., Deng, K., Lv, X., and Fang, J., "Experimental Research on Mixture Distribution of Diesel Premixed Low-Temperature Combustion," 8, 2015, doi:10.4271/2015-01-1839.

8. Musculus, M.P.B., Miles, P.C., and Pickett, L.M., "Conceptual models for partially premixed low-temperature diesel combustion," Elsevier Ltd, ISBN 0360-1285, 2013, doi:10.1016/j.pecs.2012.09.001.

9. US, D.T.T., "Advanced Combustion and Emission Control Technical Team Roadmap," 2018.

10. Buckendale, L.R., Stanton, D.W., and Stanton, D.W., "Systematic Development of Highly Efficient and Clean Engines to Meet Future Commercial Vehicle Greenhouse Gas Regulations," *SAE Int.* 2013-01-2421, 2013, doi:10.4271/2013-01-2421.

11. Prikhodko, V.Y., Curran, S.J., Parks, J.E., and Wagner, R.M., "Effectiveness of Diesel Oxidation Catalyst in Reducing HC and CO Emissions from Reactivity Controlled Compression Ignition," *SAE Int. J. Fuels Lubr.* 6(2):2013-01–0515, 2013, doi:10.4271/2013-01-0515.

12. Gehrke, S., Kovács, D., Eilts, P., Rempel, A., and Eckert, P., "Investigation of VVA-Based Exhaust Management Strategies by Means of a HD Single Cylinder Research Engine and Rapid Prototyping Systems," *SAE Tech. Pap.* 01(0587):47–61, 2013, doi:10.4271/2013-01-0587.

13. Johnson, T., "Vehicular Emissions in Review," *SAE Int. J. Engines* 9(2):2016-01–0919, 2016, doi:10.4271/2016-01-0919.

14. Schwoerer, J., Kumar, K., Ruggiero, B., and Swanbon, B., "Lost-Motion VVA Systems for Enabling Next Generation Diesel Engine Efficiency and After-Treatment Optimization," *SAE Tech. Pap.* 01(1189), 2010, doi:10.4271/2010-01-1189.

15. Guan, W., Zhao, H., Ban, Z., and Lin, T., "Exploring alternative combustion control strategies for low-load exhaust gas temperature management of a heavy-duty diesel

engine," *Int. J. Engine Res.* 146808741875558, 2018, doi:10.1177/1468087418755586.

16. Gonca, G., Sahin, B., Parlak, A., Ust, Y., Ayhan, V., Cesur, I., and Boru, B., "Theoretical and experimental investigation of the Miller cycle diesel engine in terms of performance and emission parameters," *Appl. Energy* 138:11–20, 2015, doi:10.1016/j.apenergy.2014.10.043.

17. Rinaldini, C.A., Mattarelli, E., and Golovitchev, V.I., "Potential of the Miller cycle on a HSDI diesel automotive engine," *Appl. Energy* 112(x):102–119, 2013, doi:10.1016/j.apenergy.2013.05.056.

18. Garg, A., Magee, M., Ding, C., Roberts, L., Shaver, G., Koeberlein, E., Shute, R., Koeberlein, D., McCarthy, J., and Nielsen, D., "Fuel-efficient exhaust thermal management using cylinder throttling via intake valve closing timing modulation," *Proc. Inst. Mech. Eng. Part D J. Automob. Eng.* 230(4):470–478, 2016, doi:10.1177/0954407015586896.

19. Pedrozo, V.B., May, I., Lanzanova, T.D.M., and Zhao, H., "Potential of internal EGR and throttled operation for low load extension of ethanol–diesel dual-fuel reactivity controlled compression ignition combustion on a heavy-duty engine," *Fuel* 179:391–405, 2016, doi:10.1016/j.fuel.2016.03.090.

20. Fessler, H. and Genova, M., "An Electro-Hydraulic 'Lost Motion' VVA System for a 3.0 Liter Diesel Engine," 2004(724), 2004, doi:10.4271/2004-01-3018.

21. Korfer, T., Busch, H., Kolbeck, A., Severin, C., Schnorbus, T., and Honardar, S., "Advanced Thermal Management for Modern Diesel Engines - Optimized Synergy between Engine Hardware and Software Intelligence," *Proc. Asme Intern. Combust. Engine Div. Spring Tech. Conf. 2012* 415–430, 2012, doi:10.1115/ICES2012-81003.

22. Guan, W., Pedrozo, V., Zhao, H., Ban, Z., and Lin, T., "Investigation of EGR and Miller Cycle for NOx Emissions and Exhaust Temperature Control of a Heavy-Duty Diesel Engine," *SAE Tech. Pap.*, 2017, doi:10.4271/2017-01-2227.

23. Kim, J. and Bae, C., "An investigation on the effects of late intake valve closing and exhaust gas recirculation in a single-cylinder research diesel engine in the low-load condition," *Proc. Inst. Mech. Eng. Part D J. Automob. Eng.* 230(6):771–787, 2016, doi:10.1177/0954407015595149.

24. Verschaeren, R., Schaepdryver, W., Serruys, T., Bastiaen, M., Vervaeke, L., and Verhelst, S., "Experimental study of NOx reduction on a medium speed heavy duty diesel engine by the application of EGR (exhaust gas recirculation) and Miller timing," *Energy* 76(x):614–621, 2014, doi:10.1016/j.energy.2014.08.059.

25. Benajes, J., Serrano, J.R., Molina, S., and Novella, R., "Potential of Atkinson cycle combined with EGR for pollutant control in a HD diesel engine," *Energy Convers. Manag.* 50(1):174–183, 2009, doi:10.1016/j.enconman.2008.08.034.

26. Benajes, J., Molina, S., Novella, R., and Belarte, E., "Evaluation of massive exhaust gas recirculation and Miller cycle strategies for mixing-controlled low temperature combustion in a heavy duty diesel engine," *Energy* 71:355–366, 2014, doi:10.1016/j.energy.2014.04.083.

27. Benajes, J., Molina, S., Martín, J., and Novella, R., "Effect of advancing the closing angle of the intake valves on diffusion-controlled combustion in a HD diesel engine," *Appl. Therm. Eng.* 29(10):1947–1954, 2009, doi:10.1016/j.applthermaleng.2008.09.014.

28. Sjöblom, J., "Combined Effects of Late IVC and EGR on Low-load Diesel Combustion," *SAE Tech. Pap.* 01(2878), 2014, doi:10.4271/2014-01-2878.

29. Kovács, D. and Eilts, P., "Potentials of the Miller Cycle on HD Diesel Engines Regarding Performance Increase and Reduction of Emissions," *SAE Tech. Pap. 2015-24-2440* (X), 2015, doi:10.4271/2015-24-2440.Copyright.

30. Guan, W., Pedrozo, V., Zhao, H., Ban, Z., and Lin, T., "Exploring the NOx Reduction Potential of Miller Cycle and EGR on a HD Diesel Engine Operating at Full Load," *SAE Tech. Pap.* 2018–April:1–12, 2018, doi:10.4271/2018-01-0243.

31. Kovacs, D. and Eilts, P., "Potentials of Miller Cycle on HD Diesel Engines Using a 2-Stage Turbocharging System," *SAE Tech. Pap.* 1–16, 2018, doi:10.4271/2018-01-0383.

32. Zhao, C., Yu, G., Yang, J., Bai, M., and Shang, F., "Achievement of Diesel Low Temperature Combustion through Higher Boost and EGR Control Coupled with Miller Cycle," (x), 2015, doi:10.4271/2015-01-0383.

33. Wu, B., Yu, H., Pak, P., Pei, Y., and Su, W., "Effects of Late Intake Valve Closing Timing on Thermal Efficiency and Emissions Based on a Two-stage Turbocharger Diesel Engine," *SAE Tech. Pap.* (X), 2013, doi:10.4271/2013-01-0276.

34. Millo, F., Mallamo, F., and Mego, G.G., “The Potential of Dual Stage Turbocharging and Miller Cycle for HD Diesel Engines,” *GT-Suite Users Int. Conf. Frankfurt* 2005(724), 2005, doi:10.4271/2005-01-0221.

35. Stricker, K., Kocher, L., Koeberlein, E., Alstine, D. Van, and Shaver, G.M., “Estimation of effective compression ratio for engines utilizing flexible intake valve actuation,” *Proc. Inst. Mech. Eng. Part D J. Automob. Eng.* 226(8):1001–1015, 2012, doi:10.1177/0954407012438024.

36. Pedrozo, V., “An experimental study of ethanol-diesel dual-fuel combustion for high efficiency and clean heavy-duty engines,” PhD Thesis, Brunel University London, 2017.

37. AVL., “AVL 415SE Smoke Meter,” *Prod. Guid. Graz, Austria;* 1–4, 2013.

38. Regulation No 49 – uniform provisions concerning the measures to be taken against the emission of gaseous and particulate pollutants from compression-ignition engines and positive ignition engines for use in vehicles. Off J Eur Union, 2013.

39. Zhao, H., “HCCI and CAI engines for the automotive industry,” ISBN 9781855737426, 2007.

40. Charlton, S., Dollmeyer, T., and Grana, T., “Meeting the US Heavy-Duty EPA 2010 Standards and Providing Increased Value for the Customer,” *SAE Int. J. Commer. Veh.* 3(1):101–110, 2010, doi:10.4271/2010-01-1934.

41. Hanson, R., Ickes, A., and Wallner, T., “Comparison of RCCI Operation with and without EGR over the Full Operating Map of a Heavy-Duty Diesel Engine,” *SAE Tech. Pap.* (x), 2016, doi:10.4271/2016-01-0794.

42. Pedrozo, V.B., May, I., Guan, W., and Zhao, H., “High efficiency ethanol-diesel dual-fuel combustion: A comparison against conventional diesel combustion from low to full engine load,” *Fuel* 230(February):440–451, 2018, doi:10.1016/j.fuel.2018.05.034.

43. Guan, W., Pedrozo, B., Zhao, H., Ban, Z., and Lin, T., “Miller cycle combined with exhaust gas recirculation and post–fuel injection for emissions and exhaust gas temperature control of a heavy-duty diesel engine,” *Int. J. Engine Res.* 1468087419830019, 2019, doi:10.1177/1468087419830019.

44. Authorities, A., “Acts Adopted By Bodies Created By International Agreements,” *Off. J. Eur. Union* 7–9, 2013.

45. Pedrozo, V.B. and Zhao, H., “Improvement in high load ethanol-diesel dual-fuel combustion by Miller cycle and charge air cooling,” *Appl. Energy* 210(March 2017):138–151, 2018, doi:10.1016/j.apenergy.2017.10.092.

46. Asad, U. and Zheng, M., “Exhaust gas recirculation for advanced diesel combustion cycles,” *Appl. Energy* 123:242–252, 2014, doi:10.1016/j.apenergy.2014.02.073.

47. Bobba, M., Musculus, M., and Neel, W., “Effect of Post Injections on In-Cylinder and Exhaust Soot for Low-Temperature Combustion in a Heavy-Duty Diesel Engine,” *SAE Int. J. Engines* 3(1):2010-01–0612, 2010, doi:10.4271/2010-01-0612.

48. O’Connor, J. and Musculus, M., “Post Injections for Soot Reduction in Diesel Engines: A Review of Current Understanding,” *SAE Int. J. Engines* 6(1):2013-01–0917, 2013, doi:10.4271/2013-01-0917.

49. Benajes, J., Molina, S., Novella, R., and Belarte, E., “Evaluation of massive exhaust gas recirculation and Miller cycle strategies for mixing-controlled low temperature combustion in a heavy duty diesel engine,” *Energy* 71:355–366, 2014, doi:10.1016/j.energy.2014.04.083.

50. Modiyani, R., Kocher, L., Alstine, D.G. Van, Koeberlein, E., Stricker, K., Meckl, P., and Shaver, G., “Effect of intake valve closure modulation on effective compression ratio and gas exchange in turbocharged multi-cylinder engines utilizing EGR,” *Int. J. Engine Res.* 12(6):617–631, 2011, doi:10.1177/1468087411415180.

51. Martins, M.E.S. and Lanzanova, T.D.M., “Full-load Miller cycle with ethanol and EGR: Potential benefits and challenges,” *Appl. Therm. Eng.* 90:274–285, 2015, doi:10.1016/j.applthermaleng.2015.06.086.

52. Zhao, J., “Research and application of over-expansion cycle (Atkinson and Miller) engines ??? A review,” *Appl. Energy* 185:300–319, 2017, doi:10.1016/j.apenergy.2016.10.063.

53. Kesgin, U., “Efficiency improvement and NOx emission reduction potentials of two-stage turbocharged Miller cycle for stationary natural gas engines,” *Int. J. Energy Res.* 29(3):189–216, 2005, doi:10.1002/er.1048.

Appendix A. Test cell measurement devices

Variable	Device	Manufacturer	Measurement range	Linearity/Accuracy
Speed	AG 150 Dynamometer	Froude Hofmann	0-8000 rpm	± 1 rpm
Torque	AG 150 Dynamometer	Froude Hofmann	0-500 Nm	± 0.25% of FS
Diesel flow rate (supply)	Proline promass 83A DN01	Endress+Hauser	0-20 kg/h	± 0.10% of reading
Diesel flow rate (return)	Proline promass 83A DN02	Endress+Hauser	0-100 kg/h	± 0.10% of reading
Intake air mass flow rate	Proline t-mass 65F	Endress+Hauser	0-910 kg/h	± 1.5% of reading
In-cylinder pressure	Piezoelectric pressure sensor Type 6125C	Kistler	0-300 bar	≤ ± 0.4% of FS
Intake and exhaust pressures	Piezoresistive pressure sensor Type 4049A	Kistler	0-10 bar	≤ ± 0.5% of FS
Oil pressure	Pressure transducer UNIK 5000	GE	0-10 bar	< ± 0.2% FS
Temperature	Thermocouple K Type	RS	233-1473K	≤ ± 2.5 K
Intake valve lift	S-DVRT-24 Displacement Sensor	LORD MicroStrain	0-24 mm	± 1.0% of reading using straight line
Smoke number	415SE	AVL	0-10 FSN	-
Fuel injector current signal	Current Probe PR30	LEM	0-20A	± 2 mA

Paper Correction

Dear Organizers and Reviewers,

Thank you for your kind comments and suggestions to the revised manuscript. We have modified the manuscript accordingly, and detailed corrections are listed below point by point. The paragraphs in black are the reviewers' comments, while our responses are listed in blue. All the modifications in the manuscript are highlighted in red.

We look forward to hearing from you.

Sincerely,

Wei Guan

Brunel University London

Reviewer(s)' Comments to Author:

Reviewer: 2

Comments to the Author

After reading carefully the new version of the paper I appreciate the effort carried out by the authors to provide suitable answers to my questions and, on the light of the new information added to the manuscript, I consider this version as complete and correct. Then, the quality of the manuscript fits now the high standards of IJER and my recommendation is publishing it in its current status.

Reviewer: 1

Comments to the Author

Although most of the issues from the first review have been addressed accordingly, I would at least strongly recommend the following minor revisions before publication (- the numbers refer to my original review):

(1) Concerning the novelty of your work, I understand and accept that you are attributing this to the combination of both low-load and high-load application of the measures studied. However, I still wonder if it is really necessary to explicitly stress the "originality and novelty" in the introduction, as this might provoke expectations by some readers which the paper might not be able to satisfy. My suggestion would be to simply erase the sentence "Therefore, this work includes a good novelty and originality." and leave it up to the reader to decide...

Thanks. We are agree with it and the sentence “Therefore, this work includes a good novelty and originality” has been removed from the Introduction.

(2) With respect to the influence of specific heat capacity, I agree with the statement added on page 17 ("...despite the higher heat capacity of the in-cylinder charge."); however, I am quite confused by the contradictory statement added on page 13 ("Despite the recirculation of residual gases back to the cylinder could lead to a >>lower<< specific heat..."), as the specific heat capacity of exhaust gas is higher than that of air (as correctly stated on page 17). The only factor which might contribute to a lower absolute heat capacity of the in-cylinder charge might be a reduction of the overall in-cylinder mass due to higher temperature and consequently lower density. However, the entire sentence on page 13 would make much more sense in my eyes if it started: "Despite the recirculation of residual gases back to the cylinder could lead to a higher specific heat..." [which would reduce the temperature increase obtained from compression]. Please check this, maybe this is just a misunderstanding.

Thanks. This sentence has been corrected on Page 13 accordingly.

(7) Concerning the references to literature in combination with statements or interpretations of your own investigation results, I fear you got me wrong. My point was simply to add (e.g.) ", according to the findings of [47,48]" or something similar, just in order to distinguish between your own findings and the publications you are referring to in order to substantiate your interpretation of the results. I did not mean you have to change the references you cited in the original version of the paper (so you could of course work with the previous references in case you prefer these).

Thanks for the kind suggestion. Relevant modifications have been added to distinguish between our own findings and the publications we are referring to.